ELSEVIER

Journal of Photochemistry and Photobiology B: Biology 32 (1996) 3–9

Journal of PHOTOCHEMISTRY AND PHOTOBIOLOGY B:BIOLOGY

New Trends in Photobiology (Invited Review)

Light scattering of human skin: a comparison between zinc(II)-phthalocyanine and Photofrin II®

Martin Ochsner

Physics Department, Ciba-Geigy Ltd., CH-4002 Basle, Switzerland

Received 12 February 1995; accepted 5 July 1995

Abstract

Zinc(II)-phthalocyanine is the active component of the liposomal formulation CGP 55847 which showed a high activity in photodynamic therapy studies on a variety of animal tumours (K. Schieweck et al., *SPIE Conf. Proc., 2078* (1994) 107–118).

The photophysical properties of zinc(II)-phthalocyanine have been studied in detail and compared with those of Photofrin II®, the only sensitizing agent approved so far for Phase III and IV clinical trials (M. Ochsner-Bruderer, *Inaugural Dissertation*, University of Basle, 1994). As will be shown in a series of papers, the main photophysical properties of zinc(II)-phthalocyanine are significantly better than those of Photofrin II® (M. Ochsner-Bruderer, *Inaugural Dissertation*, University of Basle, 1994).

In this paper we especially consider the effect of the absorption wavelength on the penetration of light into the human skin. The results clearly show that the longer absorption wavelength of zinc(II)-phthalocyanine causes a deeper penetration of light into the human skin as compared with Photofrin II®. In addition to this, the higher extinction coefficient (ϵ_S) lowers the zinc(II)-phthalocyanine dose required to induce a tumour necrosis.

Keywords: Photofrin II®; Zinc(II)-phthalocyanine; Photodynamic therapy; Penetration depth of light between 400 and 800 nm

1. Introduction

The possibilities of a new cancer therapy based on selective tumour destruction via intravenous injection of a photosensitizer and subsequent exposure to red light are currently being developed with great intensity in many research laboratories throughout the world. Photodynamic therapy has been used to treat approximately 10 000 patients world wide during the past 5–6 years, mostly in uncontrolled clinical studies. The only photosensitizer approved so far for Phase III and IV clinical trials is Photofrin II® from Quadra Logic Technologies, Inc. (Canada). Major drawbacks of this product are lack of chemical homogeneity, unreproducible stability, skin phototoxicity, unfavourable physicochemical properties and bad selectivity in terms of uptake and retention by tumour cells vs. normal cells [1].

Second-generation photosensitizers, including the phthalocyanines, show an increased photodynamic efficiency in the treatment of animal tumours. Their pharmacokinetic behaviours are generally more favourable and lead to an enhanced accumulation of the sensitizing agent within the tumorous tissue. Zinc(II)-phthalocyanine is a pure and chemically well-defined lipophilic substance. The absorption maximum lies at about 670 nm and its associated extinction coefficient (ϵ_S) is at least 60 times larger than that of Photofrin II® at its treatment wavelength (630 nm). The greater the ϵ_S value, the smaller is the drug dosage required to induce a cytotoxic response and the risk of provoking systemic toxic reactions is clearly diminished. As will be shown below, the longer absorption wavelength correlates with a higher penetration depth and it is therefore expected that zinc(II)-phthalocyanine causes a deeper tumour necrosis. Since the skin phototoxicity is dominated by the absorption of sunlight, a shift of the main absorption peak to higher wavelengths and a smaller overlap of the absorption spectrum of the sensitizer with the sunlight emission spectrum are expected to reduce the risk of inducing phototoxic reactions [1].

A liposomal formulation of zinc(II)-phthalocyanine for intravenous injection (CGP 55847) has been developed at Ciba-Geigy Ltd. and is currently undergoing Phase I and II clinical trials at the CHUV (Centre Hospitalier Universitaire Vaudois de Lausanne, Switzerland) in patients suffering from squamous cell carcinomas of the upper aerodigestive tract [1,2].

SSDI 1011-1344(95)07209-8

2. The liposomal formulation of zinc(II)-phthalocyanine

To permit parenteral administration of zinc(II)-phthalocyanine, a liposomal dosage form has been developed at Ciba-Geigy Ltd. in Basle (Switzerland) [2]. The liposomes were prepared from a mixture of the phospholipids 1-palmitoyl-2-oleoyl-*syn*-glycero-3-phosphocholine and 1,2-dioleoyl-*syn*-glycero-3-phospho-L-serine in a ratio of 9:1. The dye-to-lipid ratio was 1:100. The manufacturing method for this dosage form is basically a controlled solvent dilution method reproducibly yielding small liposomes of about 70–100 nm diameter in which zinc(II)-phthalocyanine is completely incorporated as monomer [2]. The liposomal zinc(II)-phthalocyanine formulation CGP 55847 contains 0.4 mg zinc(II)-phthalocyanine and 40 mg phospholipid in each vial and is freeze dried for storage. The injectable solution is prepared immediately before use by adding pyrogen-free water (2 ml per vial).

3. General remarks on the penetration depth of light

Absorption and scattering processes both reduce the light fluence as a function of the penetration depth. Based on measurements at the EPFL Lausanne [3] and on theoretical considerations [4], the intensity is mainly reduced by scattering events. The light transmission has been experimentally measured for various tissues as a function of the sample thickness and of the wavelength of the incident light [5]. Interestingly, the maximum fluence rates occurred below the surface. The position of this peak shifted more and more into the tissue with increasing wavelength.

Although large variations in the absolute values arose owing to differences in the biological material, the relative trend of the spectral dependence was quite similar. Most tissues showed an increased transparency towards higher wavelengths with a maximum penetration depth between 700 and 800 nm [5].

4. Introduction to light-scattering theories

Historically, three theories have been developed to predict the scattering and absorption properties of turbid materials such as human skin [6].

The *analytical approach* is based on a proper solution of the Maxwell equation, where the absorption and scattering characteristics of the particles are introduced via the material equation [6]. Although in principle mathematically rigorous, in practice approximations have to be made to get useful results.

In the *Monte Carlo approach* the light source is represented by a large number of single photons, for each of which the pathway through the tissue is calculated on the basis of the scattering and absorption characteristics of the material [7].

In the present approach the *radiative transfer theory* has been chosen for the prediction of the light scattering in human tissue. The transport of photon energy through a medium which contains scattering particles is calculated by solving the integrodifferential equation of Chandrasekhar [8]. For mathematical convenience the incident electromagnetic wave is assumed to be completely unpolarized. The effects of polarization could, however, be easily included through the Stokes and phase matrices [8].

5. The radiative transfer theory as applied to human skin

5.1. The integrodifferential equation of Chandrasekhar

For reasons of convenience the human skin is subdivided into slices parallel to the (x, y) plane and normal to the unit vector $\hat{z}$, which is directed inwards and perpendicular to the surface of the skin (see Fig. 1). All physical properties in each (x_1, y_1) plane are considered to be independent of the position. Based on the assumption that the treatment area is irradiated by a homogeneous light source, the light distribution within the skin (fluence rate and scattering pattern) therefore only depends on the penetration depth, i.e. on the z coordinate. Effects at the edge of the irradiation zone are neglected.

As long as the incident light beam is purely monochromatic, the integrodifferential equation of Chandrasekhar is given by [8]

$$\frac{dI(z;\theta,\phi)}{dr} = \frac{dI(z;\theta,\phi)}{dz}\cos(\theta)$$
$$= -(\sigma_a+\sigma_s)I(z;\theta,\phi)$$
$$+\sigma_s\int_0^{\pi}\int_0^{2\pi} p(\theta,\phi;\theta',\phi')I(z;\theta',\phi')\sin(\theta')\,d\phi'\,d\theta'$$

The quantity $I(z;\theta,\phi)$ (W cm^{-2} sr^{-1}) is called the specific intensity (also radiance or brightness) and is defined as a function of the penetration depth z and the angles θ and ϕ. In Fig. 1, r_0 denotes the position vector to the point (x_0, y_0, z_0) and θ and ϕ are the polar angles referred to an appropriately chosen coordinate system (x_1, y_1, z_1) through the point under investigation (x_0, y_0, z_0). Finally, the parameters σ_a (cm^{-1}) and σ_s (cm^{-1}) are the absorption and scattering coefficients respectively and $p(\theta,\phi;\theta',\phi')$ describes the phase function, i.e. the probability that a photon is scattered from the direction specified by the angles θ' and ϕ' into the (θ,ϕ) direction. Of course, the integral is taken over the whole space, i.e. over all angles θ' and ϕ'.

The left-hand side of the radiative transport equation describes the rate of change of the intensity at the point z in the direction (θ,ϕ). This rate of change is considered to be equal to the intensity lost by absorption (first term on the right-hand side) plus the intensity gained by those particles scattering the incident light from the angle (θ',ϕ') in the (θ,ϕ) direction (second term on the right-hand side).

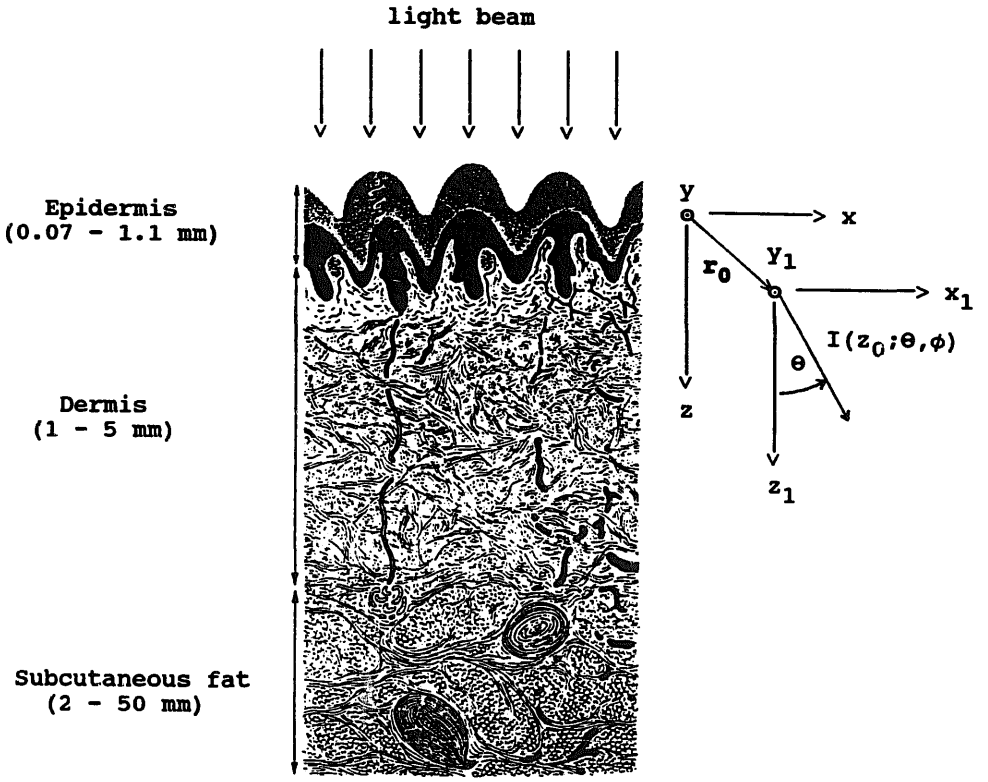

Fig. 1. Cross-section through the human skin [9]. The cartesian coordinate system (x, y, z) is superimposed on the skin. $\mathbf{r}_0$ gives the position vector of each point (x_0, y_0, z_0) from where the intensity distribution is to be determined. The polar angles θ and ϕ refer to the (x_1, y_1, z_1) coordinate system, which has its origin at the point (x_0, y_0, z_0). The azimuthal angle ϕ, which lies in the (x_1, y_1) plane, could of course not be displayed. (The data on the thickness of the skin layers were provided by Professor Dr. A. Kress, Institut für Anatomie, Basle, Switzerland.)

The radiative transfer equation is based on two assumptions. First, the medium is expected to be homogeneous. This means that any variation in the scattering and absorption properties of the medium must be on length scales much larger than the penetration depths considered. In addition, the particles are assumed to be isolated from one another, ensuring that the scattering pattern of each particle is independent of the others. As shown in Fig. 1, both assumptions are not fulfilled for human skin. The phase function $p(\theta, \phi; \theta', \phi')$ and the parameters σ_a and σ_s therefore need to be adequately chosen to represent the average scattering pattern of the ensemble.

5.2. Solution of Chandrasekhar's integrodifferential equation

5.2.1. Transformation of Chandrasekhar's integrodifferential equation to a system of coupled differential equations

Since the environment of any arbitrary point in a plane normal to the z axis is considered to be identical, solutions of the equation of transfer must be found which exhibit axial symmetry about the z axis (see Fig. 1). The intensity function $I(z; \theta, \phi)$ and the scattering integral therefore do not depend on the azimuthal angle ϕ and the equation of transfer can be written in the simplified form

$$\frac{dI(z;\theta)}{dz}\cos(\theta) = -(\sigma_a+\sigma_s)I(z;\theta) + \sigma_s 2\pi\int_0^{\pi} p(\theta;\theta')I(z;\theta')\sin(\theta')\,d\theta'$$

where $p(\theta; \theta')$ represents the phase function which has been averaged over all solid angles Ω between the (θ', ϕ') and (θ, ϕ) directions by an integration over ϕ' [8]:

$$p(\theta;\theta') = \frac{1}{2\pi}\int_0^{2\pi} p(\theta,\phi;\theta',\phi')\,d\phi'$$

By introducing the coordinate transformation $\mu = \cos(\theta)$, an alternative form of the integrodifferential equation is obtained which will subsequently be transformed into a specific system of coupled differential equations:

$$\frac{dI(z;\mu)}{dz}\mu = -(\sigma_a+\sigma_s)I(z;\mu) + \sigma_s 2\pi\int_{-1}^{1} p(\mu;\mu')I(z;\mu')\,d\mu'$$

where

$$d\mu' = \frac{d\mu'}{d\theta'} d\theta' = \frac{d}{d\theta'} \cos(\theta')\, d\theta' = -\sin(\theta')\, d\theta'$$

The integral in the radiative transfer equation can be approximated by a sum of weighted functional values at various locations of the abscissa [8,10,11]. Based on the method of Newton and Cotes, the integration interval is subdivided into equal segments [8,11]. However, Gauss showed that it is more advantageous to divide the abscissa differently, since the accuracy with which the sum predicts the real value of the integral depends intrinsically on the choice of the step size between the data points within the interval of integration $(-1, 1)$. The goal is to predict the integral as accurately as possible with the smallest number of functions required. The problem which we encounter here is basically the same as that resolved by Gauss in 1814 in deriving his formula for numerical integration (quadrature). In the gaussian formula the interval $(-1, 1)$ is divided according to the zeros (μ_j) of the Legendre polynomial $P_{2n}(\mu)$ and the integral is expressed as a sum in the form

$$\frac{dI(z; \mu_i)}{dz} \mu_i = -(\sigma_a + \sigma_s) I(z; \mu_i) + \sigma_s 2\pi \sum_{j=-n}^{n}{}' w_j p(\mu_i; \mu_j) I(z; \mu_j)$$

where $i = \pm 1, \ldots, \pm n$.

The summation over j is to be extended over all values of j, both positive and negative; there is, however, no term for $j = 0$, as indicated by the apostrophe on the sum sign (Σ'). The w_j $(j = \pm 1, \ldots, \pm n)$ are the weights for the quadrature formula based on a proper division of the interval $(-1, 1)$. It is important to point out that the inclusion of the weighting factors w_j drastically improves the accuracy of the approximation:

$$w_j = \frac{1}{P_{2n}'(\mu_j)} \int_{-1}^{1} \frac{P_{2n}(\mu)}{\mu - \mu_j} d\mu$$

$$P_{2n}'(\mu_j) = \left(\frac{d}{d\mu} P_{2n}(\mu) \right)_{\mu = \mu_j}$$

As the formula indicates, the replacement of the integral by a sum sign transforms the genuine integrodifferential equation into a set of $2n$ coupled differential equations. Apparently the accuracy of the predicted intensity distribution within the tissue not only depends on the method of choosing the step size but also grows with the number $(2n)$ of differential equations included. In other words, in making the division of the integral between -1 and 1 finer and finer, we can approach the exact solution as a limit. The number n was therefore incremented to $n = 32$ until a relative accuracy of 1 in 10^4 was reached. The finally obtained system of 64 coupled differential equations appropriately characterized the scattering behaviour at any location within the human skin.

5.2.2. Choice of the phase function $p(\mu_i; \mu_j)$

Henyey and Greenstein have introduced an analytical expression for the phase function $p_{HG}(\mu_i; \mu_j)$ to approximate Mie scattering for astrophysical studies [12]. The Henyey–Greenstein (H–G) function has found wide application in the atmospheric literature to describe light-scattering phenomena [13]. For biological systems a modified Henyey–Greenstein function $p_{m-HG}(\mu_i; \mu_j)$ which includes an additional isotropic component has been successfully used to describe the scattering of blood cells [14] and neutrophils [15]. Recent experimental work by Jacques et al. has shown that this modified H–G function describes particle light scattering in human skin quite well [16]:

$$p_{m-HG}(\mu_i; \mu_j) = \frac{1}{4\pi} \times \left(\beta + (1-\beta) \frac{1 - g_{HG}^2}{[1 + g_{HG}^2 - 2 g_{HG} \cos(\theta_i - \theta_j)]^{3/2}} \right)$$

The angles θ_i and θ_j are given by $\theta_i = \cos^{-1}(\mu_i)$ and $\theta_j = \cos^{-1}(\mu_j)$; β specifies the fraction of light scattered isotropically. When $\beta = 0$, the phase function $p_{m-HG}(\mu_i; \mu_j)$ reduces to the conventional Henyey–Greenstein function $p_{HG}(\mu_i; \mu_j)$. The parameter g_{HG} characterizes the scattering pattern and defines the anisotropy factor g, which expresses the average cosine of the phase function [16]:

$$g = \langle \cos(\theta_i - \theta_j) \rangle = (1 - \beta) g_{HG}$$

Both g and g_{HG} vary between 1 and -1. For $g = 1$ the scattering is totally peaked in the forward direction and for $g = -1$ in the backward direction. If $g = 0$, the scattering is completely isotropic.

For reasons of convenience the phase function $p_{m-HG}(\mu_i; \mu_j)$ is normalized such that the integral over all solid angles is unity:

$$\int_0^{2\pi} d\phi' \int_{-1}^{1} p_{m-HG}(\mu_i; \mu_j)\, d\mu_j = 2\pi \int_{-1}^{1} p_{m-HG}(\mu_i; \mu_j)\, d\mu_j = 1$$

6. Results and discussion

6.1. Fluence rates and polar plots of the intensity distributions

By using the absorption and scattering coefficients of Marchesini et al. [17] and their related β and g_{HG} values, the linear system of coupled differential equations could be numerically solved based on standard procedures [8,11,12]. As a result we obtained the intensities $I(z; \mu)$ at any arbitrary point in the skin and for various wavelengths in the range

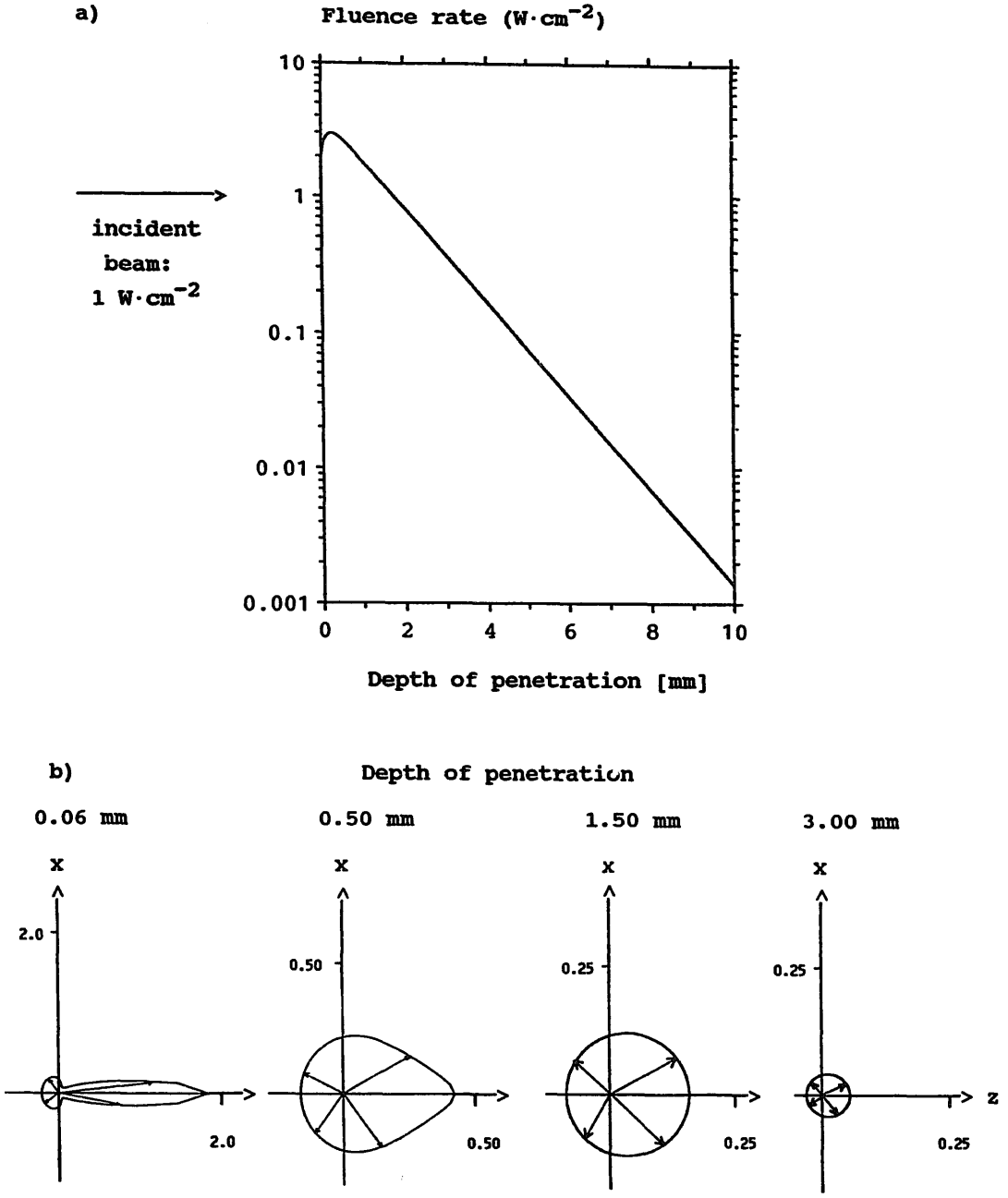

Fig. 2. (a) Fluence rate vs. penetration depth in human skin at the excitation wavelength of zinc(II)-phthalocyanine, i.e. at 670 nm. As can clearly be recognized, the maximum fluence rate occurs about 270 μm below the surface. (b) Polar plots of the radiance (W cm^{-2} sr^{-1}) at various penetration depths, showing the transition from a highly forward-peaked angular dependence near the surface to an isotropic pattern at depth ($\sigma_a = 1$ cm^{-1} and $\sigma_s = 180$ cm^{-1}).

between 400 and 800 nm. From the intensities thus determined, the fluence rates (W cm^{-2}) were finally calculated as a function of the penetration depth z:

$$F(z) = \int_0^{2\pi} d\phi \int_{-1}^{1} I(z; \mu)\, d\mu = 2\pi \int_{-1}^{1} I(z; \mu)\, d\mu$$

Of course, the integral was evaluated numerically using the gaussian quadrature formula as discussed above [8,11,12]. Even though various quadrature procedures have been developed since 1814, the gaussian formula is still superior to most of them, at least for numerical integrations in the interval between -1 and 1.

Representative of the data acquired, Fig. 2(a) shows the relative fluence rate in human skin at 670 nm as a function of the penetration depth. The graphs in Fig. 2(b) display the associated intensities as a function of the penetration depth and the angle θ_i. Strikingly near the surface the light is primarily scattered in the forward direction and becomes more and more isotropic with increasing depth of penetration. Since the absorption and scattering coefficients are 1 and 180 cm^{-1} respectively, the attenuation of the light intensity within the

a)

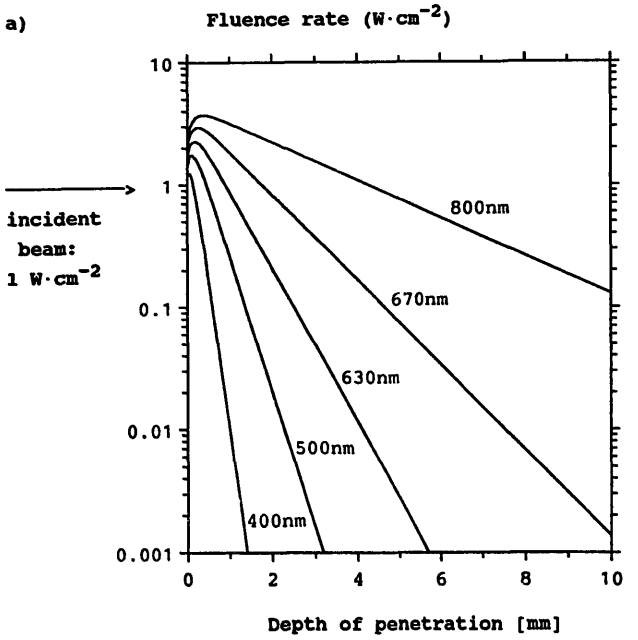

b)

λ [nm]	δ_{theory} [mm]	δ_{exp} [mm]
400	0.4	0.4
500	0.9	0.8
630	1.6	1.7
670	3.1	3.3
800	7.1	6.8

Fig. 3. (a) Fluence rates vs. penetration depth in human skin after irradiation with monochromatic light between 400 and 800 nm at an equal incident light intensity of 1 W cm^{-2}. The fluence rates at the treatment wavelengths of Photofrin II® (630 nm) and zinc(II)-phthalocyanine (670 nm) can be easily compared as a function of the penetration depth. (b) Theoretical penetration depths δ in comparison with experimental values [5,16,18,19].

tissue is dominated by scattering processes. The maximum fluence rate occurs around 270 μm below the surface, because at this point the incident light intensity is still very powerful and the volume element receives many scattered light photons from all directions. Owing to the large size of the scattering coefficient, the absorption of zinc(II)-phthalocyanine molecules located in the skin at concentrations relevant to clinical photodynamic therapy ($c_{skin} \approx 200$ nM $\rightarrow \epsilon_{ZnPc} c_{skin} \approx 0.05$ cm^{-1}; ϵ_{ZnPc}(670 nm) $\approx 270\,000$ M^{-1} cm^{-1} [20]) has a negligible effect on the light distribution within the human skin and therefore a minor influence on the penetration depth of the radiation.

The plots in Fig. 3 show the fluence rates for various wavelengths in the range between 400 and 800 nm. All results are in reasonable agreement with experimental data. The theoretically calculated exponential penetration depths δ (the 37% values of the incident fluence rate) correspond well with the experimental results (r.m.s. error about 10%–20% [16–18]). In the literature there exist a wide variety of values for the exponential penetration depth. This is due to variabilities in the physical properties of the tissues studied and to differences in the definition of the penetration depth δ. Some authors refer the 1/e value to the fluence rate just below the surface, whereas others prefer to give the inverse exponential decay constant from the point with the highest fluence rate, which is usually located 100–300 μm below the surface [5,19].

7. Preliminary results including mismatched condition at the interface

7.1. Matched vs. mismatched conditions at the interface

The presented calculations have not yet implemented the effects occurring when the light passes across a refractive index discontinuity. The graph in Fig. 1 indicates, however, that the human skin is multilayered in nature.

As discussed in detail in Refs. [6,18], the effects of reflection and transmission can be taken into account by solving the system of differential equations with regard to specific boundary conditions based on Fresnel's equation and Snell's law.

All photons which are incident at an angle θ_i (normal to the surface) on a specific interface are either reflected back into the same medium at an angle θ_r ($= -\theta_i$) or cross the boundary and penetrate the adjacent tissue section at a transmission angle θ_t as calculated from Snell's law [6,21]:

$$n_i(z_m)\ \sin(\theta_i) = n_t(z_m)\ \sin(\theta_t)$$

Here θ_i and $n_i(z_m)$ are the angle and refractive index in the medium from where the photons are coming at the location ($z = z_m$) of the considered interface, while θ_t and $n_t(z_m)$ refer to the associated constants in the medium across the plane boundary.

By neglecting any absorption of light at the interface, the reflected, $I_r(z_m;\ \theta_r)$, and transmitted, $I_t(z_m;\ \theta_t)$, specific intensities can be calculated from the incident intensity $I_i(z_m;\ \theta_i)$ via Fresnel's equation and Snell's law [6,22]:

$$I_r(z_m;\ \theta_r) = |R(z_m;\ \theta_i)|^2 I_i(z_m;\ \theta_i)$$

$$I_t(z_m;\ \theta_t) = \frac{n_t(z_m)^2[1 - |R(z_m;\ \theta_i)|^2] I_i(z_m;\ \theta_i)}{n_i(z_m)^2}$$

The reflection coefficient $R(z_m;\ \theta_i)$ depends on the polarization of the incident electromagnetic field. If the electric field vector is polarized parallel to the plane of incidence, $R(z_m;\ \theta_i)$ is identified with $R_\parallel(z_m;\ \theta_i)$, while if the field vector is polarized perpendicular to the plane of incidence, $R(z_m;\ \theta_i)$ is equal to $R_\perp(z_m;\ \theta_i)$:

$$R_\parallel(z_m;\ \theta_i) = \frac{n_i(z_m)\ \cos(\theta_t) - n_t(z_m)\ \cos(\theta_i)}{n_i(z_m)\ \cos(\theta_t) + n_t(z_m)\ \cos(\theta_i)}$$

$$R_\perp(z_m;\ \theta_i) = \frac{n_i(z_m)\ \cos(\theta_i) - n_t(z_m)\ \cos(\theta_t)}{n_i(z_m)\ \cos(\theta_i) + n_t(z_m)\ \cos(\theta_t)}$$

For a completely unpolarized wave $|R(z_m; \theta_i)|^2$ is calculated from

$$|R(z_m; \theta_i)|^2 = \tfrac{1}{2}[\,|R_{\parallel}(z_m; \theta_i)|^2 + |R_{\perp}(z_m; \theta_i)|^2]$$

As shown, it is in principle quite easy to include the effects of reflection and transmission at a given interface. However, the main problem lies in the fact that for most biological tissues, or even more specifically for the various cell layers, the indices of refraction are just not known. Published and oral presentations have quoted the use of values in the range between 1.33 and 1.55. Most of these values have just been estimated theoretically without having any experimental basis. For a wide variety of studies the index of refraction was assumed to be equal to that of water ($n = 1.33$), which is one of the major components of all mammalian organisms. Other scientists have calculated a theoretical refractive index n_{th} from the weighted elemental composition of the tissue under investigation. Recent experimental results based on the fibre optic cladding method have shown that with few exceptions the index of refraction measured for mammalian tissues at 632.8 nm is between 1.38 and 1.41 [23].

Preliminary calculations which incorporate the effects of reflection and refraction at the tissue–air interface indicate that in a medium with a high albedo ($\sigma_s/(\sigma_a+\sigma_s)$), small but, within the error limit, significant differences in the fluence rate occur near the surface of the skin. This is primarily due to photons which reach the front face and are bounced back into the skin at the tissue–air interface.

8. Conclusions

The presented data clearly indicate that the penetration depth of light is around twice as high at 670 nm as at 630 nm (see Fig. 3). As a consequence of this, we predict that the necrotic area in the tumour after irradiation with the proper wavelength is much deeper for patients who have been pretreated with zinc(II)-phthalocyanine than for patients who have received an appropriate dose of Photofrin II® [20]. The search for sensitizers which absorb at an even higher wavelength, i.e. near 800 nm, is promising, since at this wavelength the penetration depth is at least four times as high as at 630 nm.

Acknowledgement

Thanks are due to Dr. Hartmut Pauli (Ciba-Geigy Ltd., Basle) for the development of the programme used to solve the integrodifferential equations of Chandrasekhar by numerical procedures.

References

[1] M. Ochsner-Bruderer, Zinc(II)-phthalocyanine, a photosensitizer for photodynamic therapy of tumors, *Inaugural Dissertation*, University of Basle, 1994.
[2] U. Isele, P. van Hoogevest, H. Leuenberger, H.-G. Capraro and K. Schieweck, Development of CGP 55847, a liposomal Zn-phthalocyanine formulation using a controlled organic solvent dilution method, *SPIE Conf. Proc., 2078* (1994) 397–403.
[3] H. van den Bergh, personal communication, 1992.
[4] R.A.J. Groenhuis, H.A. Ferwerda and J.J. Ten Bosch, Scattering and absorption of turbid materials determined from reflection measurements 1: Theory, *Appl. Opt., 22* (1983) 2456–2462.
[5] J. Eichler, J. Knof and H. Lenz, Measurements on the depth of penetration of light (0.35–1.0 μm) in tissue, *Radiat. Environ. Biophys., 14* (1977) 239–242.
[6] A. Ishimaru, *Wave Propagation and Scattering in Random Media*, Vol. 1, Academic, New York, 1978.
[7] M.S. Patterson, B.C. Wilson and D.R. Wyman, The propagation of optical radiation in tissue I. Models of radiation transport and their application, *Lasers Med. Sci., 6* (1991) 155–168.
[8] S. Chandrasekhar, *Radiative Transfer*, Oxford University Press, New York, 1960.
[9] A. Faller, *Der Körper des Menschen*, Thieme, Stuttgart, 7th edn., 1976.
[10] W.H. Press, B.P. Flannery, S.A. Teukolsky and W.T. Vetterling, *Numerical Recipes – The Art of Scientific Computing*, Cambridge University Press, New York, 1986.
[11] K. Ebert and H. Ederer, *Computeranwendungen in der Chemie*, Verlag Chemie, Weinheim, 1983.
[12] L.G. Henyey and J.L. Greenstein, Diffuse radiation in the galaxy, *Astrophys. J., 93* (1941) 70–83.
[13] H.C. van de Hulst, *Multiple Light Scattering*, Vol. 2, Academic, New York, 1980.
[14] L. Reynolds, Optical diffuse reflectance and transmittance from an anisotropically scattering finite blood medium, *Ph.D. Dissertation*, University of Washington, Seattle, WA, 1975.
[15] D.A. Deranleau, personal communication, 1992.
[16] S.L. Jacques, C.A. Alter and S.A. Prahl, Angular dependence of HeNe laser light scattering by human dermis, *Lasers Life Sci., 1* (1987) 309–333.
[17] R. Marchesini, C. Clemente, E. Pignoli and M. Brambilla, Optical properties of in vitro epidermis and their possible relationship with optical properties of in vivo skin, *J. Photochem. Photobiol. B: Biol., 16* (1992) 127–140.
[18] S.A. Prahl, Light transport in tissue, *Ph.D. Thesis*, University of Texas, Austin, TX, 1988.
[19] S.L. Jacques, Simple theory, measurements, and rules of thumb for dosimetry during photodynamic therapy, *SPIE Conf. Proc., 1065* (1989) 100–108.
[20] K. Schieweck, H.-G. Capraro, U. Isele, P. van Hoogevest, M. Ochsner, T. Maurer and E. Batt, CGP 55847, liposome-delivered zinc(II)-phthalocyanine as a phototherapeutic agent for tumors, *SPIE Conf. Proc., 2078* (1994) 107–118.
[21] E. Hecht, *Optics*, Addison-Wesley, Menlo Park, CA, 2nd edn., 1987.
[22] M. Born, *Optik*, Springer, Berlin, 3rd edn., 1972.
[23] F.P. Bolin, L.E. Preuss, R.C. Taylor and R.J. Ference, Refractive index of some mammalian tissues using a fiber optic cladding method, *Appl. Opt., 28* (1989) 2297–2303.